analytical chemistry

Article

Identification and Quantification of Oxidation Products in Full-Length Biotherapeutic Antibodies by NMR Spectroscopy

Arthur Hinterholzer, Vesna Stanojlovic, Christof Regl, Christian G. Huber, Chiara Cabrele,* and Mario Schubert*

Cite This: *Anal. Chem.* 2020, 92, 9666−9673
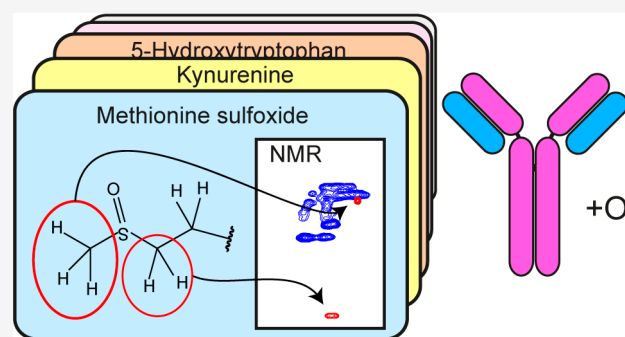
Read Online

ACCESS | Metrics & More | Article Recommendations | Supporting Information

ABSTRACT: Therapeutic proteins are an indispensable class of drugs and often therapeutics of last resort. They are sensitive to oxidation, which is of critical concern, because it can affect drug safety and efficacy. Protein oxidation, with methionine and tryptophan as the most susceptible moieties, is mainly monitored by HPLC−MS techniques. However, since several oxidation products display the same mass difference, their identification by MS is often ambiguous. Therefore, an alternative analytical method able to unambiguously identify and, ideally, also quantify oxidation species in proteins is highly desired. Here, we present an NMR-based approach to monitor oxidation in full-length proteins under denaturing conditions, as demonstrated on two biotherapeutic monoclonal antibodies (mAbs). We show that methionine sulfoxide, methionine sulfone, *N*-formylkynurenine, kynurenine, oxindolylalanine, hydroxypyrroloindole, and 5-hydroxytryptophan result in characteristic chemical shift correlations suited for their identification and quantification. We identified the five most abundant oxidation products in forced degradation studies of two full-length therapeutic mAbs and can also unambiguously distinguish oxindolylalanine from 5-hydroxytryptophan, which are undistinguishable by MS due to the same mass shift. Quantification of the abundant methionine sulfoxide by NMR and MS gave highly comparable values. These results underline the suitability of NMR spectroscopy for the identification and quantification of critical quality attributes of biotherapeutics.

Oxidation of amino acid side chains in biotherapeutics is a common alteration that can occur during production due to suboptimal processing and purification protocols as well as during prolonged storage and can lead to conformational changes or instability of proteins. Thus, the efficacy, half-life, and safety of a drug may be significantly affected.[1] The most observed oxidation product in proteins and biotherapeutics is methionine sulfoxide (Met(O)).[2−4] However, oxidation of tryptophan was also shown to have an impact on the activity, structure, and stability of biopharmaceuticals.[5−8] Since oxidation products are generally considered as critical quality attributes in biotherapeutics, tight monitoring during drug development is generally performed. Liquid chromatography together with MS are the preferred techniques to analyze post-translational modifications (PTMs). However, due to identical mass changes for structurally different oxidation products, other methods are needed for their unambiguous identification and for cross-validation of currently applied analytical methods. For this purpose, NMR spectroscopy is ideally suited, because it is the most common technique to elucidate the structure of molecules in solution.

Several recent publications have demonstrated the applicability of 2D NMR spectroscopy to detect PTMs in proteins without the necessity of isotope labeling.[9−11] This approach relies on 2D $^1H-^{13}C$ HSQC spectra of denatured proteins containing ^{13}C at natural abundance, which provides unique chemical shift pairs for the unambiguous identification of certain PTMs, e.g., succinimide,[9] *N*-glycans,[10−12] and methylated and glycated amino acids.[13] In a very recent work, we have successfully applied this method even to intact mAbs for the detection and quantification of pyroglutamate.[14] The results agreed very well with HPLC−MS so that both methods are delivering orthogonal results and can potentially be used for cross-validation. However, protein oxidation was not investigated so far by NMR spectroscopy, in particular not in denatured full-length proteins. This could be due to the large variety of oxidation products.[15−18] Denatured proteins with oxidized residues are expected to show characteristic cross-peaks in addition to those of the random-coil chemical shifts of the 20 natural amino acids.[19,20] For an unambiguous identification of
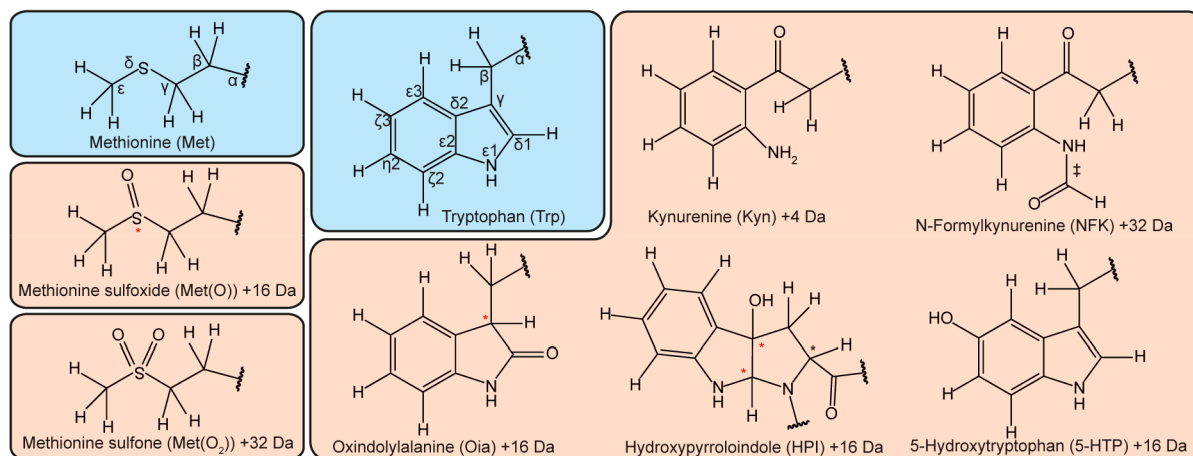
Figure 1. Possible Met and Trp oxidation products occurring in proteins. Chiral centers are indicated by an asterisk (a red asterisk represents the chiral centers generated upon the transformation of the natural residues). In the case of HPI, two stereoisomers are expected, which correspond to the *cis* or *trans* configurations of the OH group with respect to the α-carbonyl within the pyrrole ring, as previously defined by Ronsein et al.[29] In the case of *N*-formylkynurenine (NFK), two species can form, due to the *cis* and *trans* isomerization of the *N*-aryl-formamide moiety (indicated by ‡).

any oxidation product, their random-coil chemical shifts have to be assigned, typically by using model peptides containing the PTM of interest as a reference, as it was done, for example, for phosphorylated amino acids,[13,21] succinimide,[9] and pyrogluta-mate.[14]

Methionine residues are most susceptible to oxidation, leading mainly to methionine sulfoxide (Figure 1), as MS studies of a variety of biotherapeutics show.[2−4] For example, two methionine residues in the Fc/2 region of the heavy chain of rituximab (Met256, Met432) are significantly prone to H_2O_2-mediated oxidation.[4,22] Less frequent but important for certain proteins is the oxidation of tryptophan residues,[15,16] especially for mAbs.[8,23−27] Tryptophan may convert into different oxidation products, as suggested by MS studies.[6,8,23−26,28] Several oxidation mechanisms were described for tryptophan and indole-containing substances, which depend also on the oxidation conditions.[30] In any case, *N*-formylkynurenine (NFK), kynurenine (Kyn), oxindolylalanine (Oia), and hydroxytryptophans like 5-hydroxytryptophan (5HTP) have been described as the main oxidation products,[15,16,18,31−33] which are depicted in Figure 1. The chemical structures of most oxidation products in proteins are based on MS data, which is often ambiguous, because several products show identical masses (e.g., Oia and 5HTP, both characterized by a mass shift of +16 Da). Only in very few cases an unambiguous identification of a modification at a Trp residue in a protein was achieved, e.g., the detection of Kyn by X-ray crystallography in the bacterial copper binding protein MopE.[34] A comprehensive analysis of oxidation products by NMR spectroscopy has been lacking so far. Only for free 4-, 5-, and 7-HTP chemical shift assignments in D_2O were reported[35] but unrelated to peptides or proteins.

Here, we present the random-coil chemical shifts of Met(O), methionine sulfone (Met(O$_2$)), NFK, Kyn, Oia, 5HTP, and hydroxypyrroloindole (HPI) under denaturing conditions using small synthetic peptides as well as a protocol that allows the analysis of full-length proteins without the necessity of additional sample treatment, like digestion. The NMR finger-prints of these PTMs enable the unambiguous identification and quantification of methionine and tryptophan oxidation products in proteins using 2D NMR spectra as demonstrated by the two protein therapeutics rituximab and adalimumab.

EXPERIMENTAL SECTION

Peptides. Reference peptides were synthesized by solid phase peptide synthesis using Fmoc chemistry and analyzed by HPLC and MALDI-TOF-MS. H−Oia−OH, which was prepared from H−Trp−OH as described previously,[36] H−Kyn−OH, and H−5HTP−OH were Fmoc-protected as reported before[37] and coupled using a protocol described previously.[33] For experimental details, see the Supporting Information.

Forced Oxidation of Met and Trp Residues in Peptides and Proteins. To oxidze Met and Trp in reference peptides or in proteins, we used H_2O_2 at concentrations ranging from 0.35 to 1% using various incubation times at RT as described in detail in the Supporting Information.

NMR Spectroscopy. A 600 MHz Bruker Avance III HD spectrometer equipped with a $^1H/^{13}C/^{15}N/^{31}P$ quadruple-resonance probe was used to record the spectra at 298 K in 5 mm NMR tubes (ARMAR, Type 5TA) with a sample volume of 500 μL. To assign the reference peptide signals in the spectrum, the following experiments were recorded: $^1H−^{13}C$ HSQC, $^1H−^{13}C$ HMBC (hmbcgpndqf), $^1H−^1H$ TOCSY, $^1H−^1H$ COSY (cosygpppqf), $^1H−^1H$ ROESY, $^1H−^{15}N$ HSQC, $^1H−^{13}C$ HQQC,[38] and $^1H−^{13}C$ H−CO.[9] For data processing and analysis, Topspin 3.5/3.6 (Bruker) and Sparky 3.114 (T. D. Goddard and D. G. Kneller, SPARKY 3, University of California, San Francisco, USA) were used, respectively. For chemical shift referencing, approximately 0.5 mM 2,2-dimethyl-2-silapentane-5-sulfonic acid (DSS) (ARMAR Chemicals) was added to the sample after the 2D NMR measurements, and a 1D ^1H spectrum was recorded. The chemical shifts of carbon and nitrogen were referenced using the IUPAC-IUB recommended chemical shift referencing ratios Ξ of 0.251449530 (carbon) and 0.10132918 (nitrogen).[39] The chemical shift assignments are made publicly available at the BioMagResBank[40] under the accession codes 28123 (Met(O)−Gly), 28126 (Met(O)−Ala), 28127 (Met-(O−Pro), 28124 (5-HTP), 28125(Kyn), 28128 (Met(O$_2$)), 28129 (NFK), and 28130 (Oia).

Quantification of Methionine Oxidation in NMR Spectra. Quantification of induced Met(O) was performed for the NMR samples of rituximab and adalimumab, which were treated with 0.35% H_2O_2 for 30 min at RT, lyophilized, and then
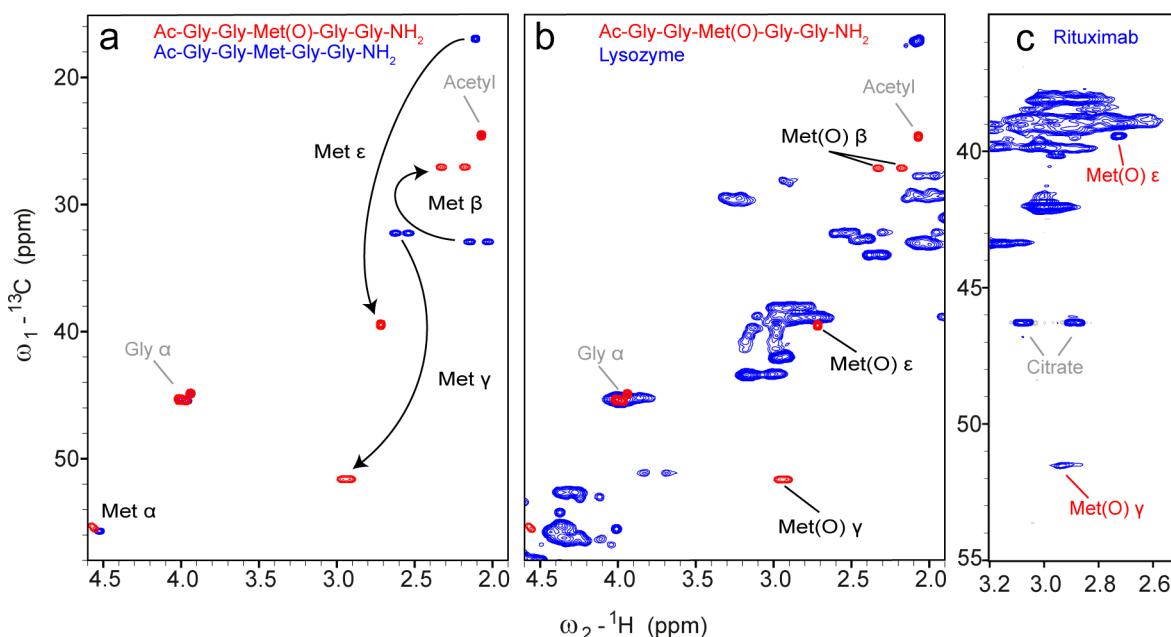
Figure 2. $^1H-^{13}C$ HSQC spectra of the reference peptides for the detection of Met(O), lysozyme, and H_2O_2-treated rituximab. (a) Overlay of the reference spectra of peptides Ac−Gly−Gly−Met(O)−Gly−Gly−NH$_2$ (red) and Ac−Gly−Gly−Met−Gly−Gly−NH$_2$ (blue) under denaturing conditions (7 M urea, pH 2.3). (b) Overlay of the spectra of the reference peptide Ac−Gly−Gly−Met(O)−Gly−Gly−NH$_2$ (red) and denatured lysozyme (blue), to identify unique chemical shifts of Met(O) that differ from the random-coil chemical shift correlations of the 20 natural amino acids. (c) $^1H-^{13}C$ HSQC spectrum of treated (0.35% H_2O_2 for 30 min at RT) rituximab (512 × 512 complex points, 104 scans, a recycle delay of 3 s, total measurement time of 2 days and 14 h) under denaturing conditions (7 M urea-d_4 in D_2O) at pH 2.3.

denatured and reduced as described previously. Four approaches (a−d) were tested and compared. **Approach a:** in the measured $^1H-^{13}C$ HSQC spectra, the Hγ−Cγ cross-peak of Met(O) was integrated (normalized to the number of methionine residues present in the mAbs; adalimumab: 10, rituximab: 12) and compared to the integrated and normalized random-coil chemical shift peaks of Cδ−Hδ of Arg (number of Arg in adalimumab: 42, in rituximab: 28), Cε−Hε of Lys (number of Lys in adalimumab: 88, in rituximab: 98), or Cβ−Hβ of Leu (number of Leu in adalimumab: 104, in rituximab: 90) (Table S1). The amino acid sequences for rituximab and adalimumab were obtained from the Web site https://www.drugbank.ca (access date 9/23/2019). **Approach b:** the Hε−Cε cross-peak of Met(O) was compared with the sum of the integrals of the Hε−Cε cross-peaks of nonoxidized Met and Met(O). **Approach c:** the integral of the Hε−Cε cross-peak of Met(O) was compared to CH_3 cross-peaks of other amino acids like Ala, Ile, and Leu. **Approach d:** the Hε−Cε cross-peak of CH_3 Met was compared to CH_3 cross-peaks of other amino acids like Ala, Ile, and Leu to obtain the amount of nonoxidized Met, from which the amount of Met(O) was then extrapolated. Approaches b and d are based on the assumption that the only oxidation product of Met is Met(O). More details and formulas regarding quantification are provided in the Supporting Information.

Quantification of Met(O) by MS. Experimental details for quantification by MS can be found in the Supporting Information. Briefly, both mAbs were trypsinized followed by peptide analysis by HPLC−ESI−Quadrupole-Orbitrap MS. Identification of modified sites was based on peptide fragmentation, and relative quantification of oxidation was based on peak areas on extracted ion current chromatograms derived from full-scan data.

■ RESULTS

Random-Coil Chemical Shifts of Synthetic Oxidation Products in Peptides. To determine the NMR signature of the previously described oxidation products of methionine and tryptophan as shown in Figure 1, we synthesized short peptides containing Met(O), Kyn, Oia, and 5HTP (Table S2). 2D NMR $^1H-^{13}C$ and $^1H-^1H$ correlations were used to obtain the ^1H and ^{13}C random-coil chemical shifts of these moieties as part of a peptide chain (Tables S3 and S4). For comparison with chemical shift data of denatured proteins, all spectra of the model peptides were recorded under denaturing conditions (7 M urea) at pH values of either 2.3 or 7.4. The acidic pH was chosen, because it aids complete denaturation of some proteins; moreover, random-coil chemical shifts at pH 2.3 had been reported previously.[19] Physiological pH (7.4) might be required for moieties that are unstable at acidic pH. To achieve maximal sensitivity and avoid disturbances of the solvent resonances, deuterated urea and D_2O were used. The chemical shifts of all investigated oxidation variants did not change significantly at the two different pH values suggesting that the presented method is also viable at pH values between 2.3 and 7.4.

The random-coil chemical shifts of Met(O) showed significantly different correlations compared to nonoxidized Met (Figure 2a). In particular, the cross-peaks of Cγ−Hγ and Cε−Hε originating of the nuclei directly adjacent to the oxidized sulfur moved to significantly different regions. Surprisingly, the chirality of the sulfur[41] did not lead to peak doubling except for a small separation of the Cα−Hα correlation (Figure 2a). Comparing these shifts with the random-coil chemical shifts of all 20 natural amino acids shows that the Hγ−Cγ cross-peaks of Met(O) are unique, well-isolated, and therefore ideally suited to unambiguously detect Met(O) in proteins (Figure 2b). The Cε−Hε cross-peak may partly overlap with Cβ−Hβ shifts of Asn; however, to resolve this degeneracy,

either spectra are recorded with higher resolution in the ^{13}C dimension (Figures 2c and S1) or a ^1H triple-quantum filtered HQQC experiment can be performed, which is selective for CH_3 groups but equally sensitive compared to an HSQC[38] (Figure S2). The HQQC experiment is suitable for an unambiguous identification of Met(O) by its unique $C\varepsilon$−$H\varepsilon$ cross-peak, without the need of high resolution in ^{13}C and thus resulting in shorter measurement time. However, its application for quantitative purposes is not recommended, since pulse imperfections and variations in scalar couplings have a much larger impact and will influence the peak intensities.

As control experiments, we analyzed if neighboring amino acids influence these characteristic chemical shift correlations (Table S5). In particular, a Pro residue at the $i + 1$ position, which is known to have the highest impact on neighboring random-coil chemical shifts,[20,42] showed only insignificant differences of the positions of the $C\gamma$−$H\gamma$ and $C\varepsilon$−$H\varepsilon$ cross-peaks (Tables S3 and S5). An Ala residue at the $i + 1$ position did not change the Met(O) chemical shifts (Table S5). This suggests that the characteristic random-coil chemical shifts for Met(O) are not impaired by the surrounding peptide sequence.

In principle, Met(O) can be further oxidized to methionine sulfone Met(O_2), but this reaction is very slow. In order to obtain NMR data of Met(O_2), the model peptide Ac−Gly−Gly−Met−Gly−Gly−NH$_2$ was treated extensively with H_2O_2 to detect possible side products apart of Met(O). Indeed, a second spin system was detected (Figure S3 and Table S6), which was identified as Met(O_2), in agreement with previously reported ^1H and ^{13}C chemical shifts.[43]

The ^1H−^{13}C random-coil chemical shift correlations of Kyn, Oia, and 5HTP showed all at least one characteristic cross-peak in the aromatic region (Figure 3). A peculiarity of Oia is that it contains a second chiral center at $C\gamma$ in addition to the chirality of $C\alpha$, and the resulting diastereomers give rise to two sets of very similar signals, e.g., at $H\beta2$ and $H\beta3$ (Table S4). In addition, keto−enol tautomerism leads to an exchange of $H\gamma$ with deuterium of the solvent so that the $H\gamma$ signal is unobservable in spectra recorded in D_2O.

NMR Characterization of Oxidation Products of Trp in a Model Peptide. Although a large variety of Trp oxidation products were described previously (Figure 1), it is unclear which variants are predominant, short-lived, or low populated. Moreover, the reactivity of the indole moiety in large, folded biomolecules strongly depends on its environment and solvent exposure as well as on the strength of the oxidant, which makes it difficult to predict the type of Trp oxidation. For example, partial conversion of the solvent-accessible Trp32 (but not Trp35) from the light chain of an mAb to Kyn and Oia or 5HTP was observed upon prolonged storage or *tert*-butylhydroperoxide treatment.[6] For another mAb (MEDI-493), it was shown that only the solvent-exposed Trp105 in the heavy chain was susceptible to oxidation: however, upon UV irradiation, the observed degradation products were Oia or 5HTP (both +16 Da) and NKF or DiOia (both +32 Da), whereas upon treatment with ozone, the major product was NFK (with Kyn, 5HTP, or Oia being only minor products).[8]

To investigate which Trp oxidation products are observable by NMR spectroscopy, we treated the peptide Ac−Gly−Gly−Trp−Gly−Gly−NH$_2$ extensively with H_2O_2 and analyzed the resulting mixture. The choice of H_2O_2 as the oxidant was made because of its frequent use to prepare oxidatively stressed protein samples for analytical purposes.[3,4,6,44] A ^1H−^{13}C fingerprint spectrum is shown in Figure 4. In addition to the
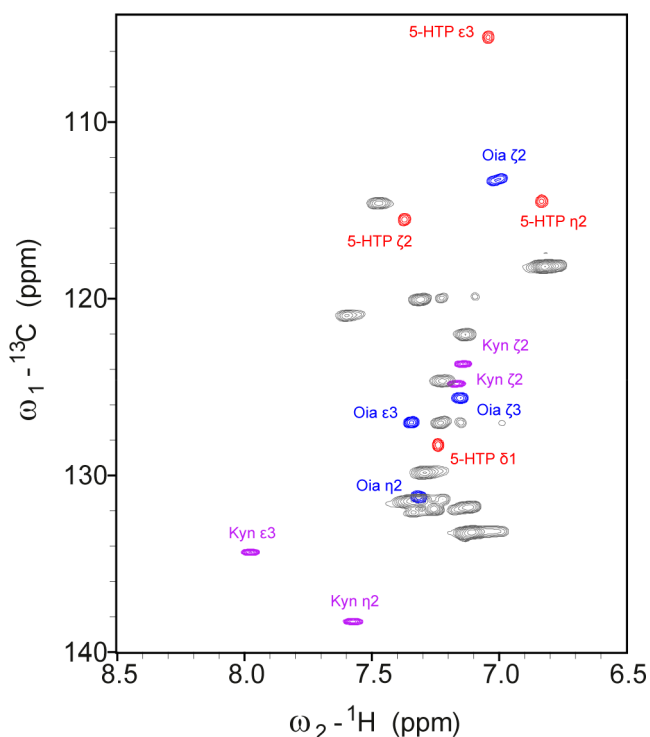

Figure 3. Overlay of the aromatic region of ^1H−^{13}C HSQC spectra of the three reference peptides containing 5-HTP (red), Kyn (purple), or Oia (blue) under denaturing conditions (7 M urea-d_4 in D_2O, pH 2.3), compared with random-coil chemical shift correlations of the natural aromatic amino acids of denatured lysozyme (gray). Several signals of the oxidation products are unique and suitable for an unambiguous identification of the different oxidation products of Trp.

expected signals of Kyn and Oia, we could identify four additional spin systems. Two of those could be assigned to NFK. These two signal sets are exchanging during the NMR experiment, as illustrated by exchange signals between their $H\zeta2$ resonances in a 2D ROESY as well as between $H\delta1$ resonances (Figure S4). The duplication of signal sets was caused by a *cis/trans* isomerization of the *N*-aryl-formamide moiety (Figure 4). Since only one cross-peak between $H\delta1$ and $C\varepsilon2$ was detected in the ^1H−^{13}C HMBC spectrum (Figure S4d), the most populated species must be the one in which $H\delta1$ and $C\varepsilon2$ are in *trans*, for which a higher value of $^3J_{H\delta1C\varepsilon2}$ is expected compared to the *cis*-$H\delta1/C\varepsilon2$ configuration. This is further supported by the ^1H and ^{13}C chemical shifts of the formyl group, which are more downfield for the *cis* form, according to previous NMR studies of *N*-formyl-group-containing compounds.[45,46] The downfield chemical shift of $H\zeta2$ at 8.14 ppm can be explained in the case of *cis*-NFK by the proximity to the formyl oxygen. The other two similar sets of signals matched previously reported chemical shifts of the two diastereomers of hydroxypyrroloindole (HPI), which the authors named *trans*- and *cis*-HPI (Figure 4).[29] However, the formation of HPI, which involves a bond between the backbone nitrogen and the former $C\delta1$ of Trp, was so far only reported as an oxidation product of the free amino acid tryptophan. Now, we show that this tricyclic product can be formed also when the tryptophan is incorporated into a peptide backbone. Interestingly, we observed that the intensities of the NFK signals decreased over time, while those of Kyn increased. A spectrum recorded immediately after the oxidation treatment contained mainly NFK and barely Kyn, whereas a sample measured after
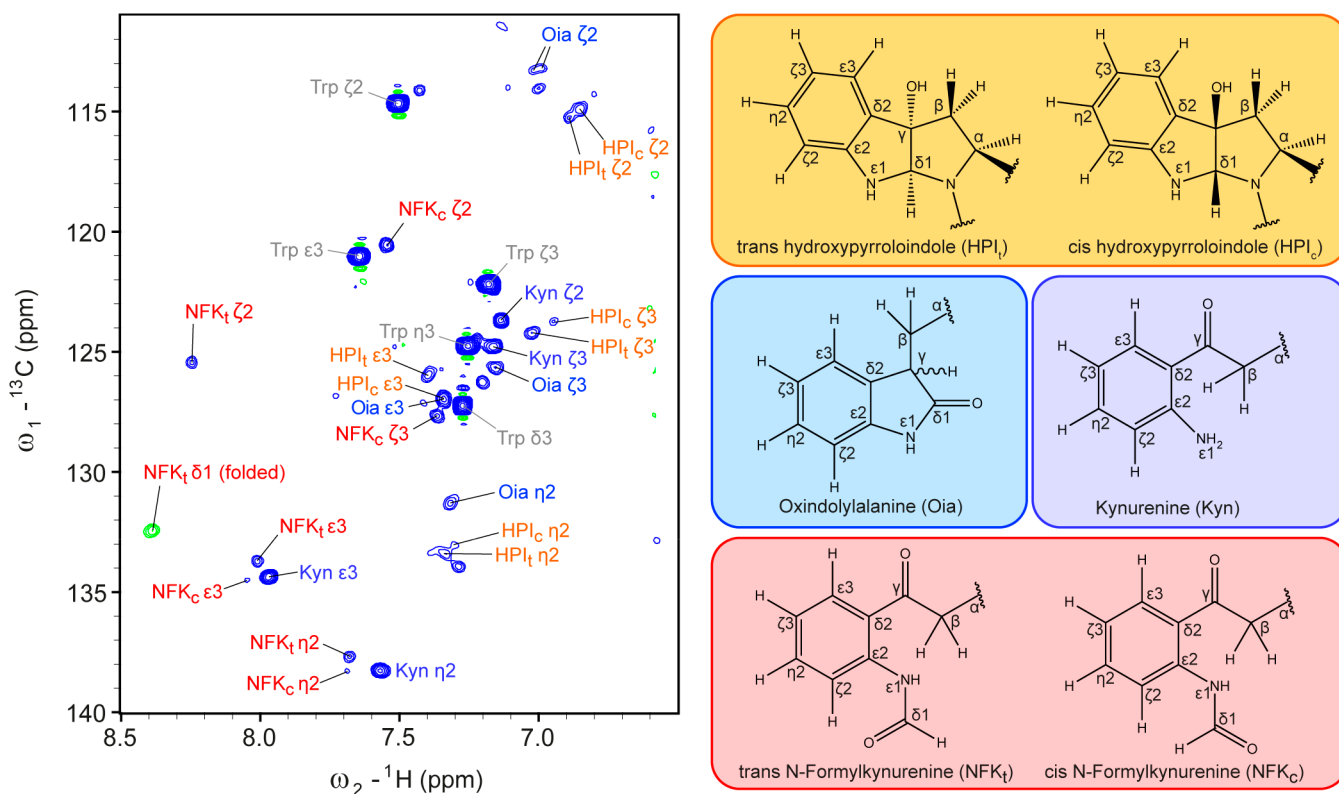
Figure 4. $^1H-^{13}C$ HSQC spectrum of the aromatic region of the Trp-containing peptide Ac—Gly—Gly—Trp—Gly—Gly—NH$_2$ under denaturing conditions (7 M urea-d_4 in D$_2$O) after treatment with 1% H$_2$O$_2$ for 5 h, dialysis, and lyophilization. Four different oxidation products of Trp could be detected and are shown on the right. For HPI, Oia, and NFK, two sets of shifts can be observed due to different stereoisomers.

several days displayed predominantly Kyn signals. This indicates a conversion of NFK into Kyn over time (Figure S5). To our surprise, we did not observe any signals matching to 5HTP nor even vaguely to other HTP species.[35] However, we cannot rule out that 5HTP is formed under different oxidation conditions.

Identification of Oxidation Products in Biotherapeutics Using 2D NMR. In order to detect Met(O) in full-length proteins, we chose the two mAbs rituximab and adalimumab as model systems. For positive controls, we introduced methionine oxidation by treating the proteins with H$_2$O$_2$. All protein samples were buffer exchanged, lyophilized, and subsequently denatured by using 7 M urea-d_4 and tris(2-carboxyethyl)-phosphine hydrochloride (TCEP) as a reducing agent. These conditions resulted in a completely denatured state even for intact mAbs both at acidic and neutral conditions. Therefore, no digestion and fragment separation was necessary using our approach. The H$_2$O$_2$-treated proteins (30 min at room temperature, 0.35% H$_2$O$_2$), investigated at the two pH conditions (2.3 and 7.4), revealed characteristic Cγ—Hγ and Cε—Hε cross-peaks indicative for Met(O) (Figures 2c and S6). Signals indicating the presence of Met(O$_2$) and Trp oxidation products were not observed after these conditions were applied. However, by performing extended oxidation under denaturing conditions (1% H$_2$O$_2$ for 25 h in the formulation buffer, measured in 7 M urea and 11 mM TCEP), it was possible to detect Met(O$_2$) (Figures S7 and S8) and the Trp oxidation products Oia, and Kyn. In particular, Cε3—Hε3 and Cζ3—Hζ3 cross-peaks of Oia and weak signals of Cε2—Hε2 and Cη2—Hη2 of Kyn were detected in a 2D $^1H-^{13}C$ HSQC spectrum (Figure S9a) of rituximab. Interstingly, in a sample treated for more than five days, Kyn but not Oia was observed (Figure S9c,d). Weak

NFK signals were also detected, which, however, dissapeared over time.

Quantification of Met(O) in (H$_2$O$_2$-Treated) mAbs. NMR spectroscopy is, in principle, a quantitative method as long as sufficiently long recycle delays ensure the restoration of equilibrium magnetization and as long as signals do not overlap. For the quantification of the most abundant oxidation product Met(O) using 2D $^1H-^{13}C$ HSQC spectra of rituximab and adalimumab treated with H$_2$O$_2$, we evaluated several approaches that were based on the following considerations: (i) The well-isolated CH$_3$ group of nonoxidized Met is sharp and well-suited for quantification, whereas the CH$_3$ group of Met(O) is located close to other random-coil correlations, mainly of Asn. Therefore, due to the difficulty of integrating overlapping signals, the Cε—Hε integral of Met(O) might have a larger error. However, very high resolution in the ^{13}C dimension results in an isolated signal and thus overcomes this challenge and provides an excellent handle for quantification (Figure S10). (ii) The signal of CH$_2$ at Cγ of Met(O) is well-isolated, in contrast to the corresponding signal of nonoxidized Met. However, it is quite weak, which results in large integration errors. (iii) Suitable reference signals for cross-peak integration were chosen by taking into account the different multiplicities and slightly different $^1J_{CH}$ scalar couplings so that integrals of CH$_2$ were only compared to other CH$_2$ signals, and integrals of CH$_3$ were only compared to other CH$_3$ signals. Therefore, the resulting approaches to obtain the fraction of Met(O) were as follows (a–d): (a) the integral of Cγ—Hγ of Met(O) was compared to those of Lys Cε—Hε, Arg Cδ—Hδ, and Leu Cβ—Hβ signals; (b) the integral of CH$_3$ of Met(O) (Cε—Hε cross-peak) was divided by the sum of the integrals of Met(O) and Met methyl signals

(the latter have the advantage of being more intense than the methylene signals); (c) alternatively, the integral of CH$_3$ of Met(O) was compared to each of the methyl groups of Ile, Ala, and Leu; (d) in addition, we tested an indirect approach for the quantification of Met(O), based on the typically intense CH$_3$ signal of nonoxidized Met Cε−Hε, which was compared to the methyl groups of Ile, Ala, and Leu under the assumption that methionine sulfoxide is the only modification of Met occurring in the protein. Further details and applied equations for calculating the Met(O) fractions and their associated errors are given in the Supporting Information.

The results of all approaches applied to rituximab and adalimumab treated with H$_2$O$_2$ are summarized in Table 1. For

Table 1. Quantification of Induced Met(O) in Rituximab and Adalimumab Treated with 0.35% H$_2$O$_2$ for 30 min at RT

cross-peaks used for quantification[a]	rituximab Met(O) (%)	adalimumab Met(O) (%)
a: Met(O) Cγ/Hγ compared to		
Arg Cδ/Hδ	14.3 ± 1.9[c]	15.3 ± 1.0[c]
Leu Cβ/Hβ	18.7 ± 4.6[c]	17.3 ± 1.9[c]
Lys Cε/Hε	16.2 ± 2.3[c]	14.7 ± 1.6[c]
b:[b] Met(O) Cε/Hε compared to		
Met Cε/Hε	18.3 ± 1.0[c]	19.1 ± 1.2[c]
c: Met(O) Cε/Hε compared to		
Ala Cβ/Hβ	18.3 ± 3.8[c]	19.3 ± 0.5[c]
Ile Cδ1/Hδ1	18.6 ± 1.3[c]	19.6 ± 0.7[c]
Ile Cγ2/Hγ2	17.8 ± 1.8[c]	19.7 ± 1.2[c]
Leu Cδ1/Hδ1	18.1 ± 0.9[c]	18.7 ± 0.5[c]
Leu Cδ2/Hδ2	18.2 ± 1.5[c]	18.7 ± 0.8[c]
d:[b] Met Cε/Hε compared to		
Ala Cβ/Hβ2	18.4 ± 3.8[c]	18.3 ± 4.7[c]
Ile Cδ1/Hδ1	16.9 ± 3.6[c]	17.4 ± 5.5[c]
Ile Cγ2/Hγ2	20.8 ± 5.8[c]	16.8 ± 7.4[c]
Leu Cδ1/Hδ1	19.1 ± 2.1[c]	21.0 ± 4.6[c]
Leu Cδ2/Hδ2	18.7.4 ± 4.8[c]	21.1 ± 5.6[c]
MS	17.9 ± 1.3	21.3 ± 1.2

[a]^{1}H−^{13}C HSQC spectra used for quantification shown in Figure S6. [b]Based on the assumption that Met(O) is the only oxidation product of Met. [c]Error determined using eqs 3, 5, and 7 (see Supplementary Methods).

both mAbs, all approaches gave comparable values. However, the quantification based on CH$_2$ groups showed larger errors than the other direct approaches based on CH$_3$ groups. This can be explained by the weaker Met(O) CH$_2$ signals and the associated lower accuracy of their integrals. Neither was Met(O$_2$) detected nor was the sum of the integrals of Met and Met(O) smaller than expected, indicating Met(O) was the only PTM of Met. However, an important parameter for a reliable quantification is a sufficiently long recycle delay. In our case, the recycle delay of 3 s was sufficient, whereas 2 s led to a reduction of the Hε−Cε signal of nonoxidized Met, which resulted in a smaller total integral of all methionine species and, consequently, in overestimation of Met(O) using quantification methods (b) and (d).

The quantification of oxidation of the same samples was also performed with MS (Tables 1 and S7). The relative quantification of total methionine oxidation showed that on average 17.9% of all methionine residues in rituximab and 21.3% of all methionine residues in adalimumab were oxidized, which is in the same range as the values obtained by NMR. The relative

oxidation rates of every single methionine residue are provided in Table S7. As previously reported, the methionine residues Met256 and Met432 in the Fc domain of the mAbs were most prone to oxidation[22] and, indeed, showed the highest percentage of oxidation. Figure S11 depicts one example of the identification and relative quantification by MS: oxidized and nonoxidized peptide species were identified, based on the fragment ion spectra (Figure S11b,c) and subsequently relatively quantified based on peak areas of the full-scan mass spectra (Figure S11a). It should be noted that consistent quantification data were only obtained when the sample was kept under argon atmosphere during the sample preparation steps in order to exclude oxidation by atmospheric oxygen.

■ DISCUSSION

The presented random-coil chemical shift assignment of the most important oxidation products of Met and Trp (Figure 1) enables a straightforward and unambiguous identification of these modifications in proteins under denaturing conditions. Due to standardized conditions, the random-coil chemical shifts are generally applicable, independent of the NMR instrument and without the necessity of reference peptides. Owing to the flexibility of the protein chain in the unfolded state, our approach results in narrow line widths even for large proteins. With this method, there is per se no size limit, and large proteins like full-length mAbs can be analyzed, as long as it is possible to denature them. This has been demonstrated here by using rituximab and adalimumab as model systems. In contrast to MS studies that, in general, require the digestion of mAbs for the detection of Met(O),[4,47,48] we can use intact proteins. Middle-down or bottom-up approaches have the disadvantage of laborious sample preparation, which can also lead to artifacts due to the formation of additional degradation products. With regard to oxidation, the atmospheric oxygen can significantly increase Met(O) formation during long incubation times. As an orthogonal and complementary approach to MS, we propose to use a straightforward NMR-based protocol for the investigation of the oxidation of small proteins, like lysozyme, as well as of large ones, like mAbs, at different pH values. This is especially suited for forced degradation studies generating modifications identical to those that are spontaneously formed during the lifetime of a drug but typically with much higher amounts (>10%). Our method can unambiguously assess the identity of the oxidation products, which is very important in the case of chemical modifications characterized by the same mass difference (e.g., Oia and HTP). In this way, ambiguous assignment or even overestimation of side products with identical masses can be avoided. Since our NMR protocol relies on the random-coil chemical shift fingerprints of modified residues, it provides the chemical identity but not the position of the modification. Therefore, additional MS measurements would be necessary, which, again, underlines the complementarity of the NMR and MS approaches for the complete characterization of protein degradation products. Besides the application to large proteins, like mAbs, also small-to-medium-size therapeutic peptides are ideally suited for our NMR-based approach. These peptides may be particularly susceptible to spontaneous chemical changes during production and storage, due to the lack of a well-defined three-dimensional structure. Because of the small molecular weight of peptides and higher achievable concentrations, it seems even feasible to use NMR for product quality control.

Although the amount of protein required, the detection limit, and the relatively long measurement time might represent some limitations to the NMR approach, it should be considered that biotherapeutics are usually produced in large scale, and thus, the quantities required for NMR are accessible. The required NMR measurement time will depend on the sensitivity of the spectrometer, obviously being dramatically shortened with higher fields. Similarly, the detection limit reflects the type of equipment utilized for the NMR measurements: for example, we have recently shown that the lowest detectable amount of pyroglutamate (pGlu) in mAbs was about 55 μM by using a 600 MHz spectrometer with a cryogenic probe (TCI) and 2 days measurement time.[14] Therefore, we assume that, also in the case of Met and Trp oxidation products, the limit of detection will be in the two-digit micromolar range. However, the use of higher field magnets in combination with cryogenic probes will allow reaching even lower limits of detections, as shown by Peng et al., who could detect glycosylation in mAb fragments down to about 10% by using an 850 MHz spectrometer with a cryogenic probe with a measurement time of 11 h.[10]

To quantify Met(O) by NMR spectroscopy, we propose that the most reliable approach is the one based on the integrals of the methyl group of Met(O) and of other isolated methyl groups of the protein (approach (c)). This requires very high resolution in the ^{13}C dimension to prevent overlap of the Met(O) methyl signal with nearby random-coil signals. Depending on the reference methyl groups, the obtained Met(O) amount varied by approximately 2%, which is within the error estimated for each value. Alternatively, the integrals of the well-isolated Cγ/ Hγ2 + Hγ3 methylene group signals of Met(O) and of other isolated methylene signals of the protein can be used (approach a) even at lower resolution, but the error of the Met(O) fraction will be higher (approximately 4%) due to the weaker intensity of the methylene group of Met(O). The other two approaches ((b) and (d)), which are based on the assumption that Met(O) is the only oxidation product of Met and thus that the sum of the integrals of Met and Met(O) represent all methionine species, are less recommended, because they are sensitive to the presence of any other oxidation products of methionine. Another factor to consider is that a sufficiently long recycle delay is crucial for the experiment. In case of the quantification of Met(O), a recycle delay of 3 s was required to obtain reliable quantification results.

CONCLUSION

Here, we provide for the first time the complete NMR characterization of the seven most relevant oxidation products potentially occurring in proteins under denaturing conditions (detailed summary in Figure S12). These chemical shift assignments revealed for each of the species unique cross-peaks in 2D fingerprint spectra, allowing an unambiguous identification of these chemical moieties in any protein under denaturing conditions. The applicability of this method in a biopharmaceutical context is demonstrated in a forced degradation study of two biotherapeutic mAbs through the identification of the oxidation products, but its use in quality control of peptide pharmaceuticals is feasible as well. The characteristic chemical shift fingerprints enable an unambiguous identification even for cases, which are undistinguishable by MS. The fact that we could identify the most common oxidized species in such large proteins like rituximab and adalimumab (treated) shows how powerful these chemical shift assignments are in combination with ^{1}H–^{13}C spectra under denaturing conditions.

ASSOCIATED CONTENT

ⓢ Supporting Information

The Supporting Information is available free of charge at https://pubs.acs.org/doi/10.1021/acs.analchem.0c00965.

2D ^{1}H–^{13}C HSQC spectra, chemical shift assignment tables, HPLC and MS characterization data, Met(O) quantification data, and supplementary methods (PDF)

AUTHOR INFORMATION

Corresponding Authors

Mario Schubert – *Christian Doppler Laboratory for Innovative Tools for Biosimilar Characterization and Department of Biosciences, University of Salzburg, 5020 Salzburg, Austria;* orcid.org/0000-0003-0278-4091; Email: mario.schubert@sbg.ac.at

Chiara Cabrele – *Christian Doppler Laboratory for Innovative Tools for Biosimilar Characterization and Department of Biosciences, University of Salzburg, 5020 Salzburg, Austria;* orcid.org/0000-0002-7550-6896; Email: chiara.cabrele@sbg.ac.at

Authors

Arthur Hinterholzer – *Christian Doppler Laboratory for Innovative Tools for Biosimilar Characterization and Department of Biosciences, University of Salzburg, 5020 Salzburg, Austria;* orcid.org/0000-0003-0006-6547

Vesna Stanojlovic – *Department of Biosciences, University of Salzburg, 5020 Salzburg, Austria;* orcid.org/0000-0001-5924-9634

Christof Regl – *Christian Doppler Laboratory for Innovative Tools for Biosimilar Characterization and Department of Biosciences, University of Salzburg, 5020 Salzburg, Austria*

Christian G. Huber – *Christian Doppler Laboratory for Innovative Tools for Biosimilar Characterization and Department of Biosciences, University of Salzburg, 5020 Salzburg, Austria;* orcid.org/0000-0001-8358-1880

Complete contact information is available at:
https://pubs.acs.org/10.1021/acs.analchem.0c00965

Author Contributions

M.S., C.C., and A.H. designed the experiments. V.S. synthesized the reference peptides and noncommercially available building blocks. A.H. and M.S. performed the NMR experiments and assigned the NMR resonances. C.R. performed and interpreted the MS experiments. C.G.H. supervised the MS analysis. M.S., C.C., and A.H. wrote the manuscript. All authors reviewed and approved the manuscript.

Notes

The authors declare the following competing financial interest(s): The salary of A.H. is fully funded and C.G.H.'s salary is partly funded by the Christian Doppler Laboratory for Biosimilar Characterization, which is partly supported by Novartis GmbH and Thermo Fisher Scientific. The authors declare no other competing financial interest.

■ REFERENCES

(1) Torosantucci, R.; Schöneich, C.; Jiskoot, W. *Pharm. Res.* **2014**, *31* (3), 541−553.

(2) Davies, M. J. *Biochim. Biophys. Acta, Proteins Proteomics* **2005**, *1703* (2), 93−109.

(3) Forstenlehner, I. C.; Holzmann, J.; Toll, H.; Huber, C. G. *Anal. Chem.* **2015**, *87* (18), 9336−9343.

(4) Regl, C.; Wohlschlager, T.; Holzmann, J.; Huber, C. G. *Anal. Chem.* **2017**, *89* (16), 8391−8398.

(5) Gao, X.; Ji, J. A.; Veeravalli, K.; Wang, Y. J.; Zhang, T.; Mcgreevy, W.; Zheng, K.; Kelley, R. F.; Laird, M. W.; Liu, J.; Cromwell, M. *J. Pharm. Sci.* **2015**, *104* (2), 368−377.

(6) Hensel, M.; Steurer, R.; Fichtl, J.; Elger, C.; Wedekind, F.; Petzold, A.; Schlothauer, T.; Molhoj, M.; Reusch, D.; Bulau, P. *PLoS One* **2011**, *6* (3), e17708.

(7) Liu, D.; Ren, D.; Huang, H.; Dankberg, J.; Rosenfeld, R.; Cocco, M. J.; Li, L.; Brems, D. N.; Remmele, R. L. *Biochemistry* **2008**, *47* (18), 5088−5100.

(8) Wei, Z.; Feng, J.; Lin, H.-Y.; Mullapudi, S.; Bishop, E.; Tous, G. I.; Casas-Finet, J.; Hakki, F.; Strouse, R.; Schenerman, M. A. *Anal. Chem.* **2007**, *79* (7), 2797−2805.

(9) Grassi, L.; Regl, C.; Wildner, S.; Gadermaier, G.; Huber, C. G.; Cabrele, C.; Schubert, M. *Anal. Chem.* **2017**, *89* (22), 11962−11970.

(10) Peng, J.; Patil, S. M.; Keire, D. A.; Chen, K. *Anal. Chem.* **2018**, *90* (18), 11016−11024.

(11) Schubert, M.; Walczak, M. J.; Aebi, M.; Wider, G. *Angew. Chem., Int. Ed.* **2015**, *54* (24), 7096−7100.

(12) Unione, L.; Lenza, M. P.; Ardá, A.; Urquiza, P.; Laín, A.; Falcón-Pérez, J. M.; Jiménez-Barbero, J.; Millet, O. *ACS Cent. Sci.* **2019**, *5* (9), 1554−1561.

(13) Conibear, A. C.; Rosengren, K. J.; Becker, C. F. W.; Kaehlig, H. *J. Biomol. NMR* **2019**, *73* (10−11), 587−599.

(14) Hinterholzer, A.; Stanojlovic, V.; Cabrele, C.; Schubert, M. *Anal. Chem.* **2019**, *91* (22), 14299−14305.

(15) Ehrenshaft, M.; Deterding, L. J.; Mason, R. P. *Free Radical Biol. Med.* **2015**, *89*, 220−228.

(16) Finley, E. L.; Dillon, J.; Crouch, R. K.; Schey, K. L. *Protein Sci.* **1998**, *7* (11), 2391−2397.

(17) Grassi, L.; Cabrele, C. *Amino Acids* **2019**, *51*, 1409−1431.

(18) Nakagawa, M.; Watanabe, H.; Kodato, S.; Okajima, H.; Hino, T.; Flippen, J. L.; Witkop, B. *Proc. Natl. Acad. Sci. U. S. A.* **1977**, *74* (11), 4730−4733.

(19) Schwarzinger, S.; Kroon, G. J.A.; Foss, T. R.; Wright, P. E.; Dyson, H. J. *J. Biomol. NMR* **2000**, *18* (1), 43−48.

(20) Wishart, D. S.; Bigam, C. G.; Holm, A.; Hodges, R. S.; Sykes, B. D. *J. Biomol. NMR* **1995**, *5* (1), 67−81.

(21) Bienkiewicz, E. A.; Lumb, K. J. *J. Biomol. NMR* **1999**, *15*, 203−206.

(22) Gaza-Bulseco, G.; Faldu, S.; Hurkmans, K.; Chumsae, C.; Liu, H. *J. Chromatogr. B: Anal. Technol. Biomed. Life Sci.* **2008**, *870* (1), 55−62.

(23) Pavon, J. A.; Xiao, L.; Li, X.; Zhao, J.; Aldredge, D.; Dank, E.; Fridman, A.; Liu, Y.-H. *Anal. Chem.* **2019**, *91* (3), 2192−2200.

(24) Folzer, E.; Diepold, K.; Bomans, K.; Finkler, C.; Schmidt, R.; Bulau, P.; Huwyler, J.; Mahler, H.-C.; Koulov, A. V. *J. Pharm. Sci.* **2015**, *104* (9), 2824−2831.

(25) Li, Y.; Polozova, A.; Gruia, F.; Feng, J. *Anal. Chem.* **2014**, *86* (14), 6850−6857.

(26) Wong, C.; Strachan-Mills, C.; Burman, S. *J. Chromatogr. A* **2012**, *1270*, 153−161.

(27) Sreedhara, A.; Lau, K.; Li, C.; Hosken, B.; Macchi, F.; Zhan, D.; Shen, A.; Steinmann, D.; Schöneich, C.; Lentz, Y. *Mol. Pharmaceutics* **2013**, *10* (1), 278−288.

(28) Domingues, M. R. M.; Domingues, P.; Reis, A.; Fonseca, C.; Amado, F. M. L.; Ferrer-Correia, A. J. V. *J. Am. Soc. Mass Spectrom.* **2003**, *14* (4), 406−416.

(29) Ronsein, G. E.; Oliveira, M. C. B.; Miyamoto, S.; Medeiros, M. H. G.; Di Mascio, P. *Chem. Res. Toxicol.* **2008**, *21* (6), 1271−1283.

(30) Zhang, X.; Foote, C. S.; Khan, S. I. *J. Org. Chem.* **1993**, *58* (1), 47−51.

(31) Maskos, Z.; Rush, J. D.; Koppenol, W. H. *Arch. Biochem. Biophys.* **1992**, *296* (2), 514−520.

(32) Simat; Steinhart. *J. Agric. Food Chem.* **1998**, *46* (2), 490−498.

(33) Todorovski, T.; Fedorova, M.; Hennig, L.; Hoffmann, R. *J. Pept. Sci.* **2011**, *17* (4), 256−262.

(34) Helland, R.; Fjellbirkeland, A.; Karlsen, O. A.; Ve, T.; Lillehaug, J. R.; Jensen, H. B. *J. Biol. Chem.* **2008**, *283* (20), 13897−13904.

(35) van den Berg, E. M. M.; Jansen, F. J. H. M.; de Goede, A. T. J. W.; Baldew, A. U.; Lugtenburg, J. *Recl. Trav. Chim. Pays-Bas* **1990**, *109* (4), 287−297.

(36) Labroo, R. B.; Cohen, L. A. *J. Org. Chem.* **1990**, *55* (16), 4901−4904.

(37) Raillard, S. P.; Mann, A. D.; Baer, T. A. *Org. Prep. Proced. Int.* **1998**, *30* (2), 183−186.

(38) Kessler, H.; Schmieder, P.; Köck, M.; Reggelin, M. *J. Magn. Reson.* **1991**, *91* (2), 375−379.

(39) Markley, J. L.; Bax, A.; Arata, Y.; Hilbers, C. W.; Kaptein, R.; Sykes, B. D.; Wright, P. E.; Wüthrich, K. *J. Biomol. NMR* **1998**, *12*, 1−23.

(40) Ulrich, E. L.; Akutsu, H.; Doreleijers, J. F.; Harano, Y.; Ioannidis, Y. E.; Lin, J.; Livny, M.; Mading, S.; Maziuk, D.; Miller, Z.; Nakatani, E.; Schulte, C. F.; Tolmie, D. E.; Kent Wenger, R.; Yao, H.; Markley, J. L. *Nucleic Acids Res.* **2007**, *36*, D402−8.

(41) Lee, B. C.; Gladyshev, V. N. *Free Radical Biol. Med.* **2011**, *50* (2), 221−227.

(42) Schwarzinger, S.; Kroon, G. J. A.; Foss, T. R.; Chung, J.; Wright, P. E.; Dyson, H. J. *J. Am. Chem. Soc.* **2001**, *123* (13), 2970−2978.

(43) Takizawa, Y.; Fukushima, H.; Usui, T.; Yoshihara, N.; Takizawa, J. *J. Jpn. Oil. Chem. Soc.* **1992**, *41* (5), 428−430.

(44) Holzmann, J.; Hausberger, A.; Rupprechter, A.; Toll, H. *Anal. Bioanal. Chem.* **2013**, *405* (21), 6667−6674.

(45) Hu, X.; Zhang, W.; Carmichael, I.; Serianni, A. S. *J. Am. Chem. Soc.* **2010**, *132* (13), 4641−4652.

(46) Quintanilla-Licea, R.; Colunga-Valladares, J.; Caballero-Quintero, A.; Rodríguez-Padilla, C.; Tamez-Guerra, R.; Gómez-Flores, R.; Waksman, N. *Molecules* **2002**, *7* (8), 662−673.

(47) Huang, L.-J.; Chiang, C.-W.; Lee, Y.-W.; Wang, T.-F.; Fong, C.-C.; Chen, S.-H. *J. Chromatogr. B: Anal. Technol. Biomed. Life Sci.* **2016**, *1032*, 189−197.

(48) Mo, J.; Yan, Q.; So, C. K.; Soden, T.; Lewis, M. J.; Hu, P. *Anal. Chem.* **2016**, *88* (19), 9495−9502.